Overcoming PLK1 inhibitor resistance by targeting mevalonate pathway to impair AXL-TWIST axis in colorectal cancer

Sonia Solanes-Casado [a], Arancha Cebrián [a,*], María Rodríguez-Remírez [b], Ignacio Mahíllo [c], Laura García-García [a], Anxo Río-Vilariño [a], Natalia Baños [a], Guillermo de Cárcer [d], Ana Monfort-Vengut [d], Víctor Castellano [e], Maria Jesús Fernández-Aceñero [f], Jesús García-Foncillas [a,*,1], Laura del Puerto-Nevado [a,*,1]

[a] Translational Oncology Division, Oncohealth Institute, IIS - Fundación Jiménez Díaz University Hospital (IIS-FJD, UAM), Madrid, Spain
[b] Department of Oncology, Clínica Universitaria de Navarra, Pamplona, Spain
[c] Department of Statistics, IIS - Fundación Jiménez Díaz University Hospital (IIS-FJD, UAM), Madrid, Spain
[d] Cell Cycle & Cancer Biomarkers Group, Instituto de Investigaciones Biomédicas "Alberto Sols" (IIBm) CSIC-UAM, 28029 Madrid, Spain
[e] Department of Pathology, Fundación Jiménez Díaz University Hospital (UAM), Madrid, Spain
[f] Department of Pathology, Hospital Clínico San Carlos, Instituto de Investigación Sanitaria del Hospital Clínico San Carlos (IdISSC), Madrid, Spain

ARTICLE INFO

ABSTRACT

New therapeutic targets are revolutionizing colorectal cancer clinical management, opening new horizons in metastatic patients' outcome. Polo Like Kinase1 (PLK1) inhibitors have high potential as antitumoral agents, however, the emergence of drug resistance is a major challenge for their use in clinical practice. Overcoming this challenge represents a hot topic in current drug discovery research.

BI2536-resistant colorectal cancer cell lines HT29$_R$, RKO$_R$, SW837$_R$ and HCT116$_R$, were generated *in vitro* and validated by IG$_{50}$ assays and xenografts models by the T/C ratio. Exons 1 and 2 of PLK1 gene were sequenced by Sanger method. AXL pathway, Epithelial-to-Mesenchymal transition (EMT) and Multidrug Resistance (MDR1) were studied by qPCR and western blot in resistant cells. Simvastatin as a re-sensitizer drug was tested *in vitro* and the drug combination strategies were validated *in vitro* and *in vivo*.

PLK1 gene mutation R136G was found for RKO$_R$. AXL pathway trough TWIST1 transcription factor was identified as one of the mechanisms involved in HT29$_R$, SW837$_R$ and HCT116$_R$ lines, inducing EMT and upregulation of MDR1. Simvastatin was able to impair the mechanisms activated by adaptive resistance and its combination with BI2536 re-sensitized resistant cells *in vitro* and *in vivo*.

Targeting the mevalonate pathway contributes to re-sensitizing BI2536-resistant cells *in vitro* and *in vivo*, raising as a new strategy for the clinical management of PLK1 inhibitors.

1. Introduction

Colorectal cancer (CRC) was the third most commonly diagnosed neoplasia in the last 2020 and it ranked the second place in mortality according to the Globocan database [1]. Spite surveillance strategies and early diagnosis have increased the survival at initial-stages; the metastatic disease remains a difficult entity to deal with. There are many efforts aimed to understand the mechanisms associated with tumor progression and drug response. To date, CRC classifications based on different criteria, laterality and microsatellite stability [2,3]. presence of KRAS mutations [4] or molecular subtypes based on genes differential expression [5], together with the tumor stage, lead the therapeutical pathway in order to establish the most effective therapy for patients [6,7].

In the last few decades, as a result of the continuous research, there have been an increasing number of targeted therapies approved for the

treatment of metastatic CRC, enhancing the benefit of standard chemotherapy [8,9]. Likewise, new therapeutic targets are discovered steadily to contribute in the enhancement of the therapeutic strategies and outcome of CRC patients [10]. Many of them are designed to disturb the cell cycle given that many tumor-associated processes are linked to an abnormal regulation of protein kinases involved in the progression throughout the cell division cycle. That is the case of Polo Like-Kinase 1 (PLK1), a key serin-threonin kinase responsible for G2-M transition and mitosis entrance [11], which overexpression has been reported in several types of tumors, correlating with progression disease, metastasis and poor prognosis [12,13]. PLK1 is activated by Aurora Kinase A (AURKA), carrying on with the pathway until the dephosphorylation of the complex Cyclin B - CDK1, one of the transcription factors responsible of mitosis entry [10,11]. PLK1 is formed by two domains: C-terminal polo-box domain (PBD) and N-terminal catalytic domain (CD), being the latter the responsible for the PLK1 function in mitosis since is where the ATP binding site is located, necessary to phosphorylate its substrate, the phosphatase CDC25c [14,15].

Given PLK1 critical function in mitotic regulation, this kinase has been the subject of extensive research [16]. As a consequence, a large number of PLK1 inhibitors have been developed. Most of them are ATP competitors, small molecules that join to ATP binding site in CD blocking ATP union and substrate phosphorylation [17,18]. Some of these ATP competitors are BI2536, BI6727 (Volasertib), GSK461364, Onvansertib or Rigosertib. They have been already tested in phase I-III clinical trials for solid tumors (breast cancer, head and neck cancer, melanoma, sarcoma, ovarian, prostate and pancreas cancer) as well as hematological malignancies (acute myeloid leukemia and non-Hodking linfoma) with varying degrees of responses [19].

Spite of their potential, effectiveness of such agents is markedly limited by the emergence of drug resistance due to, among others, frequent mutations at the ATP-binding pocket [20] or other adaptive mechanisms that enable the prematurely exit mitosis or mitotic slippage [21]. These mechanisms could be responsible for the limited success of these molecules both alone and combined with adjuvant and neo-adjuvant chemotherapy in the clinic [22].

Taking into account the potential of these inhibitors for CCR patient's management, it looks reasonable to characterize the adaptive resistance mechanisms to reformulate the use of these molecules by their combination with other drugs and overcome the activated mechanisms. As a result, our manuscript described not only some of the mechanisms activated during the PLK1 inhibitor BI2536 resistance in a cohort of CRC cell lines, but also, the design of *in vitro* and *in vivo* combinatory strategies for overcoming the mitotic slippage.

This manuscript contributes to enhance the knowledge regarding resistance mechanisms, a hot topic in current drug discovery research and participates in re-positioning PLK1 inhibitors as first line in the new horizons for CCR metastatic patients' treatment.

2. Methods

2.1. Cell culture and inhibitors

CRC cell lines HT29, RKO, SW837 and HCT116 were obtained from American Type Culture Collection (ATCC) and cultured in RPMI 1640 medium (Gibco, Waltham, MA, USA) supplemented with 10% FBS (Gibco, Waltham, MA, USA) and 1% of mixture Penicillin (100 U/mL) – Streptomycin (100 μg/mL), at 37 °C in controlled humidity and 5% CO_2.

PLK1 inhibitor BI2536 (HY-50698), Simvastatin (HY-17502) and R428 (HY-15150) were obtained from MedChemExpress LLC (Monmouth Junction, NJ, USA). BI2536 was dissolved in DMSO 100% (Sigma Aldrich, San Luis, MO, USA), diluted in RPMI at different concentrations for *in vitro* assays and in 80% HCl 0,1 N, NaCl 0,9%, 20% PEG400 for *in vivo* experiments. R428 was dissolved in DMSO 100% (Sigma Aldrich, San Luis, MO, USA) and diluted in RPMI at different concentrations. Simvastatin was activated with EtOH 100% and NaOH 1 N; diluted in

RPMI for *in vitro* assays and diluted in 10% DMSO, 40% PEG300, 5% TWEEN 80% and 45% NaCl 0,9% for *in vivo* experiments.

2.2. Inhibition growth (IG) assays

IG assays were performed with the Cell Counting Kit-8 (CCK-8; Sigma Aldrich, San Luis, MO, USA). Between 3 and 10×10^3 cells / well were seeded in a 96-well plate and incubated for 24 h. Then, BI2536 was added to the plate in a concentration range from 5 nM to 2000 nM. 72 h later, CCK-8 was added to each well (20 μL) and incubated for 2 h at 37 °C and 5% CO_2. The absorbance was measured at 450 nm in a spectrometer plate reader. Each experiment was developed in triplicate and mean value for absorbance data in each concentration point was used for calculations. The IG_{50} value for each cell line was obtained by a function which fits a 5-parameter logistic model: $y = B + (T - B) / [1 + 10^{b(xmid-x)}]^S$.

where B and T are the lower and upper asymptotes, b is the slope, x_{mid} is the value of x at which the inflexion point occurs, and s is a co-efficient of skewness. Curves were developed by plotting the mean values derived from the experimental triplicates.

2.3. Resistance induction

IG_{50} values were used as starting concentrations to generate BI2536 resistant cell lines. Briefly, cells were seeded and treated with BI2536; after 4 days, drug was withdrawn and fresh medium was added for 3 days; after this time cells were treated again with the same dose and repeated the procedure for 2 cycles. This protocol was repeated continuously with a progressive increase of the drug dose until cells were considered resistant.

2.4. In vitro assays

Sensitive and resistant cells were seeded in 6-well plates in a concentration between 15 and 30×10^4 cells / well. After 24 h, BI2536, Simvastatin or R428 were added to the wells and cell pellets were collected 48 h later and stored at −20 °C. Samples obtained were used for proteins and mRNA expression analysis. Each experiment was developed in triplicate and expressed as mean ± standard deviation (SD).

2.5. PLK1 sequencing

Genomic DNA was isolated from each cell line using NucleoSpin® Tissue (MACHEREY-NAGEL, Düren, Germany). Exon 1 (FW: GGCTCCACCGGCGAAAGAG; RW: TAGCAGCTCCCAGAGCCAAGA) and exon 2 (FW: TCTCTCCTGGAGCTGCACAAG; RW: GCATCTGTAGGCAA-GATACTGACTTG) of PLK1 were amplified as follow: 95 °C 5′, 35x (95 °C 30′′, 59 °C 30′′ for exon 1 or 55 °C 30′′ for exon 2, and 72 °C 45′′) and 4 °C infinite. PCR product was purified with QIAquick PCR Purification Kit (Qiagen, Hilden, Germany), and sent to sequence to Macrogen (https://www.dna.macrogen.com/) (Geumcheon-gu, Seoul, Korea) by Sanger Sequencing.

2.6. Multidrug resistance assay

MDR1 activity was assessed using the Multidrug Resistance Assay Kit (Cayman Chemical, Ann Arbor, MI, USA), following the manufacturer's instructions. Calcein AM signal was measured by fluorescence in a plate reader using excitation and emission wavelengths of 485 nm and 535 nm, respectively.

Additionally, Hoechst 33342 Staining Dye Solution (ab228551, Abcam, Cambridge, UK) was used to stain nuclei of live cells to normalize the signal of Calcelin AM with cell numbers in wells. It was added to the plate at the same time that Calcein AM, and measured with excitation and emission wavelengths of 355 nm and 465 nm,

respectively. Results were presented as the percentage of Calcein AM / Hoechst ratio Each experiment was developed in triplicate and expressed as mean ± standard deviation (SD).

2.7. Western blotting

Proteins were isolated from cellular pellets with RIPA buffer supplemented with protease (Roche, Basilea, Switzerland) and phosphatase (PhosSTOP, Roche, Basilea, Switzerland) inhibitors following manufacturer's instructions. Total protein was quantified with the commercial kit Pierce™ BCA Protein Assay Kit (Thermo Fisher-Scientific, Waltham, MA, USA).

Proteins were prepared at the same concentration and resolved by electrophoresis gel SDS-PAGE, transferred into a nitrocellulose membrane and blocked for 1 h with non-fat dried milk powder 5% in Saline Tris-buffer with Tween 20 (TTBS). Membranes were washed with TTBS.

Primary antibodies were incubated overnight at 4 °C: PLK1 (Cell Signaling; #4513), phosphoThr210 PLK1 (Cell Signaling; #9062), PARP (Cell Signaling; #9542), AXL (Cell Signaling; #8661), E-Cadherin (BD Bioscience Transduction Lab.; #67A4), Vimentin (BD Bioscience Transduction Lab; #550513), MDR1 (Cell Signaling; #12683), β-Actin (Cell Signaling; #3700), GAPDH (Cell Signaling; #97166). Then, membranes were washed with TTBS and incubated with secondary antibody anti-rabbit or anti-mouse peroxidase-conjugated. The signal was detected using enhanced chemoluminescence (ECL Prime; Amersham Pharma Biotech Inc., Little Chalfont, UK) in the Amersham Imager 600 (GE Healthcare, Chicago, IL, USA). The result quantification was performed with ImageJ software. Each experiment was developed in triplicate and expressed as mean ± standard deviation (SD).

2.8. Quantitative PCR

RNA isolation from cellular pellets and pulverized tumors was performed using the commercial kit NucleoSpin® RNA (MACHEREY-NAGEL, Düren, Germany) according to manufacturer's instructions, and quantified with NanoDrop 2000 spectrophotometer (Thermo Fisher-Scientific, Waltham, MA, USA). cDNA was synthesized with High Capacity cDNA Reverse Transctiption kit (Applied Biosystem, Foster City, CA, USA) from 1 µL of 200 ng/µL of total RNA following manufacturer's instructions.

Applied Biosystems 7500 Fast Real-Time PCR System was used to perform quantitative real-time PCR. PCR reaction mix was prepared with 0,25 µL of each TaqMan probe, using the problem probe FAM marked, and housekeeping probe VIC marked, 5 µL of Universal PCR Master Mix (Applied Biosystems, Foster City, CA, USA) and 3,5 µL of nuclease-free water. Previously generated cDNA was added to each well, in a proportion 9 µL of mix and 1 µL of cDNA, analyzing a triplicate for each sample or condition in a 96-well plate.

The genes explored were *AXL* (Hs01064444_m1), *TWIST1* (Hs01675818_s1), *ABCB1* (Hs00184500_m1), *Vimentin* (Hs00958111_m1), and all of them were normalized using *RPLP0* (Hs99999902_m1) (Applied Biosystems, Foster City, CA, USA).

Each experiment was developed in triplicate and expressed as mean ± standard deviation (SD).

2.9. Tumor Xenograft models

Female athymic nude-Foxn1nu 5–6 week-old mice were used from Envigo RMS (Indianapolis, IN, USA). Animals were housed in the Animal Model Core Facility of IIS–Fundacion Jimenez Diaz (ES28079000089). All animal procedures and experimental protocols were approved by the Ethical Animal Research Committee at IIS-Fundacion Jimenez Diaz (Madrid, Spain) and were also conducted in accordance with institutional standards (Reference n°: PROEXP 024–15), which fulfilled the requirements established by the Spanish government and the European Community (Real Decreto R.D. 53/2003).

2.9.1. Xenograft development

Subcutaneous injection of 2×10^6 cells diluted in 200 µL of mixture 1:1 PBS and Matrigel (Corning Inc., NY, USA) in subscapular location was performed from each of the 4 lines (parental/resistant). When tumors reached a volume of 150 mm^3, mice were randomized into vehicle, BI2536 and Simvastatin (only in re-sensitization model) branches with 4–6 mice per group.

BI2536 was administered intraperitoneally in a 20 mg/kg dose, twice a week, and Simvastatin was administered intraperitoneally in a 5 mg/kg dose, three times a week. All treatments were administered during 21 days. Tumor volumes were measured every 2 days with a caliper and calculated with the equation (a x b^2)/2, where "a" is the largest tumor diameter and "b" the perpendicular tumor diameter. At endpoint animals were sacrificed with carbon dioxide (CO$_2$) inhalation and tumors were snap-frozen in liquid nitrogen, stored at −80 °C and pulverized for further quantitative PCR assays.

2.9.2. Antitumor evaluation and T/C ratio

To evaluate antitumor activity of BI2536 and Simvastatin T/C ratio was applied, where "T" is the mean of tumor volume of treated group at day 21, and "C" the mean of tumor volume of control group at day 21. This ratio expressed as percentage is an antitumor indicator; less than 42%, the treatment shows antitumor activity or drug sensitivity, and more than 42% is considered not showing antitumor activity, or drug resistance [23]. Graphics express the mean volume ± standard deviation (SD) for each time point and experimental condition.

2.10. Statistical analysis

Statistical analyses were performed using SPSS software version 20.0 (SPSS Inc, Chicago, IL, USA). Results were expressed as mean ± standard deviation (SD) of the triplicate of each experiment. Comparison between groups was evaluated by Mann-Whitney test.

3. Results

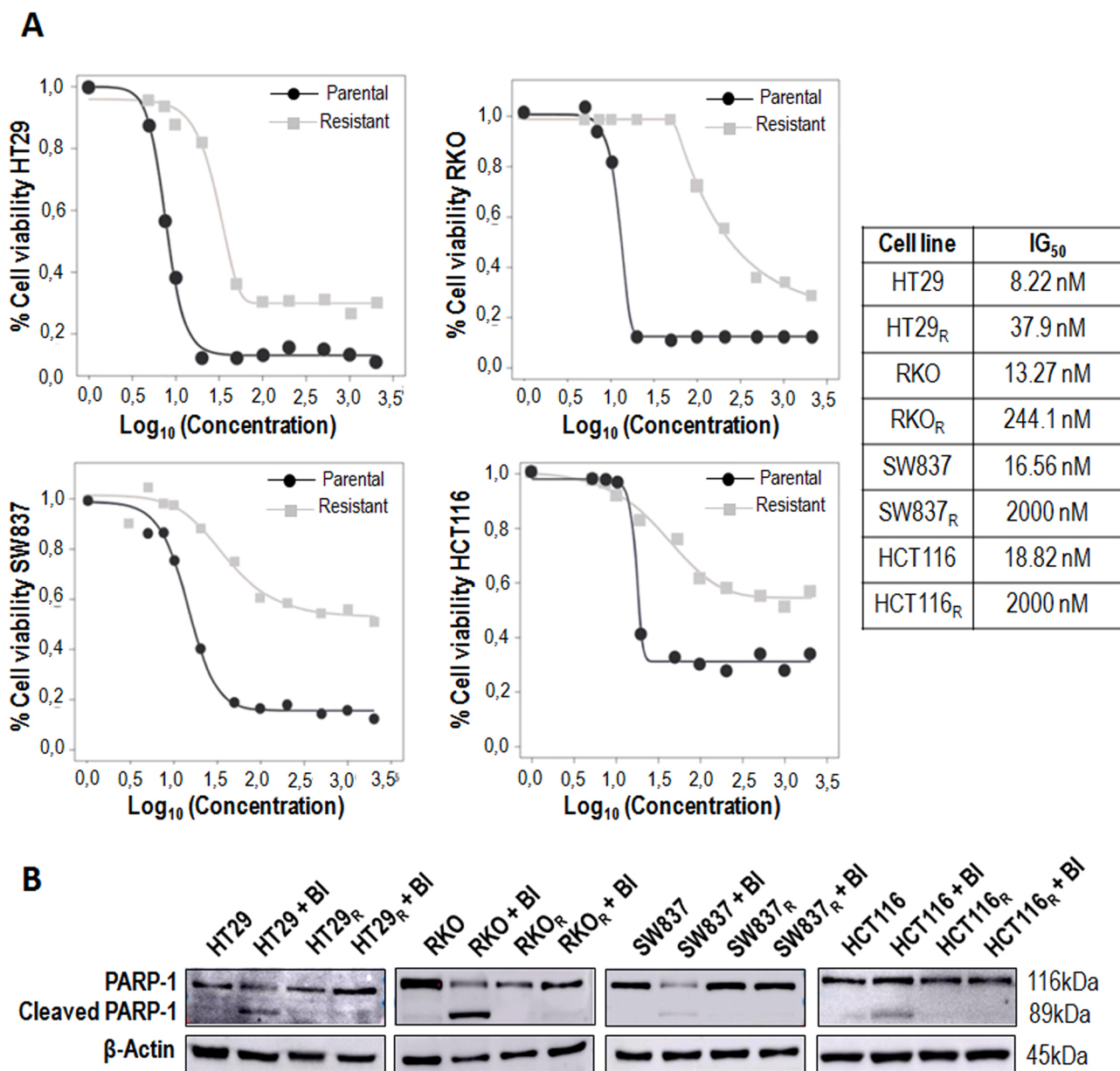## 3.1. BI2536-resistant cell lines generation and validation

To induce BI2536-resistance, we selected a set of colorectal cell lines with different molecular profiles based on their PLK1 total protein levels, PLK1 activation ratio (phosphoThr210PLK1/PLK1), *KRAS* mutational status, and molecular subtype (microsatellite stability or suppressor phenotype, and microsatellite instability or mutated phenotype) (Supplementary Figure 1) [24]. In view of these molecular characteristics, cell lines selected were HT29, RKO, SW837 and HCT116.

To establish the BI2536-resistant cell lines, selected cells were cultured with increasing concentrations of PLK1 inhibitor over a period ranged from 9 to 18 months. Starting dose of BI2536, corresponding to concentrations below each IG$_{50}$ value (HT29 8,22 nM; RKO 13,27 nM; SW837 16,56 nM and HCT116 18,82 nM) was gradually increased up to 55 nM under conditions of at least an 80% survival rate after 24 h of culture.

Resistant cells (HT29$_R$, RKO$_R$, SW837$_R$ and HCT116$_R$) showed between 4 and 120-fold greater resistance to BI2536 compared to their parental ones (HT29, RKO SW837 and HCT116). IG$_{50}$ values were calculated for each resistant cell line: HT29$_R$ 37,9 nM; RKO$_R$ 244,1 nM; SW837$_R$ 2000 nM and HCT116$_R$ 2000 nM (Fig. 1A).

Cleavage of PARP by caspases is considered to be a hallmark of apoptosis. Thus, to validate the acquired BI2536-resistance the presence of PARP and cleaved PARP were assessed by western blot in parental and resistant cell lines. As expected, the experiments confirmed the presence of cleaved PARP in treated parental cell lines, and its absence in treated resistant lines (Fig. 1B). These results indicated that BI2536 only induced apoptosis in parental cells confirming the resistant behavior of HT29$_R$, RKO$_R$, SW837$_R$ and HCT116$_R$.

Xenograft models were also developed to evaluate the acquired

A

Cell line	IG_{50}
HT29	8.22 nM
$HT29_R$	37.9 nM
RKO	13.27 nM
RKO_R	244.1 nM
SW837	16.56 nM
$SW837_R$	2000 nM
HCT116	18.82 nM
$HCT116_R$	2000 nM

B

Fig. 1. In vitro validation of BI2536-induced resistance in CRC cell lines. (A) Inhibition Growth curves for parental (black line) and resistant (grey line) cell lines adjusted to a logistic function. Graphs show the percentage of cell viability versus $\log_{10}$ concentration of BI2536 after 72 hrs of treatment. The table displays the estimated concentrations for a response of 0.5 (IG_{50} values). (B) PARP-1 and cleaved PARP-1 assessment by western blot after 72 hrs of BI2536 treatment. β-actin is used as a control loading. BI2536 doses used for this experiment were above IG_{50} concentration of parental cells (16 nM for HT29/HT29$_R$, 30 nM for RKO/RKO$_R$, SW837/SW837$_R$ and HCT116/HCT116$_R$).

resistance by comparing the effect of BI2536 on the growth of tumors derived from parental or resistant lines (Fig. 2). Differences between treated parental and resistant models were observed. T/C ratios indicated that parental cells were highly sensitive to BI2536 (HT29 12%, RKO 36%, SW837 23% and HCT116 11%) in comparison to resistant models (HT29$_R$ 80%, RKO$_R$ 119%, SW837$_R$ 64% and HCT116$_R$ 59%), which achieved T/C ratios over 42% confirming the *in vivo* BI2535 resistance.

3.2. PLK1 sequencing in parental and resistant cell lines

There are some evidences which associate the presence of mutations in the sequence encoding the ATP binding pocket of PLK1 with acquired resistance to PLK1 inhibitors. These mutations provoke specific amino acid changes, such as L59W, F183L or R136G, that correlate with a loss

of affinity for the inhibitors and could be a possible resistance mechanism.

Mutation screening in exon 1 and 2 of *PLK1* were carried out in all parental and resistant cell lines. In case of HT29, SW837 and HCT116 cell lines neither parental nor resistant phenotype carried any mutation. However, a heterozygous mutation was observed in the RKO resistant cell line when it was compared with the parental cell line. A change of Adenine to Guanine at nucleotide 421 which produces an Arginine-Glycine replacement in the peptide sequence (R136G). This mutation has been previously described in PLK1 inhibitors resistance and seems to modify the inhibitor affinity to its union site (Supplementary Figure 2A).

To test if the presence of this mutation could also affect to other PLK1 inhibitors efficacy, we performed IG$_{50}$ curves for other inhibitors using the RKO$_R$ cell line. The BI2536-resistant mutated cell line, RKO$_R$, showed cross-resistance to other PLKis. Values of BI6727 (Volasertib)
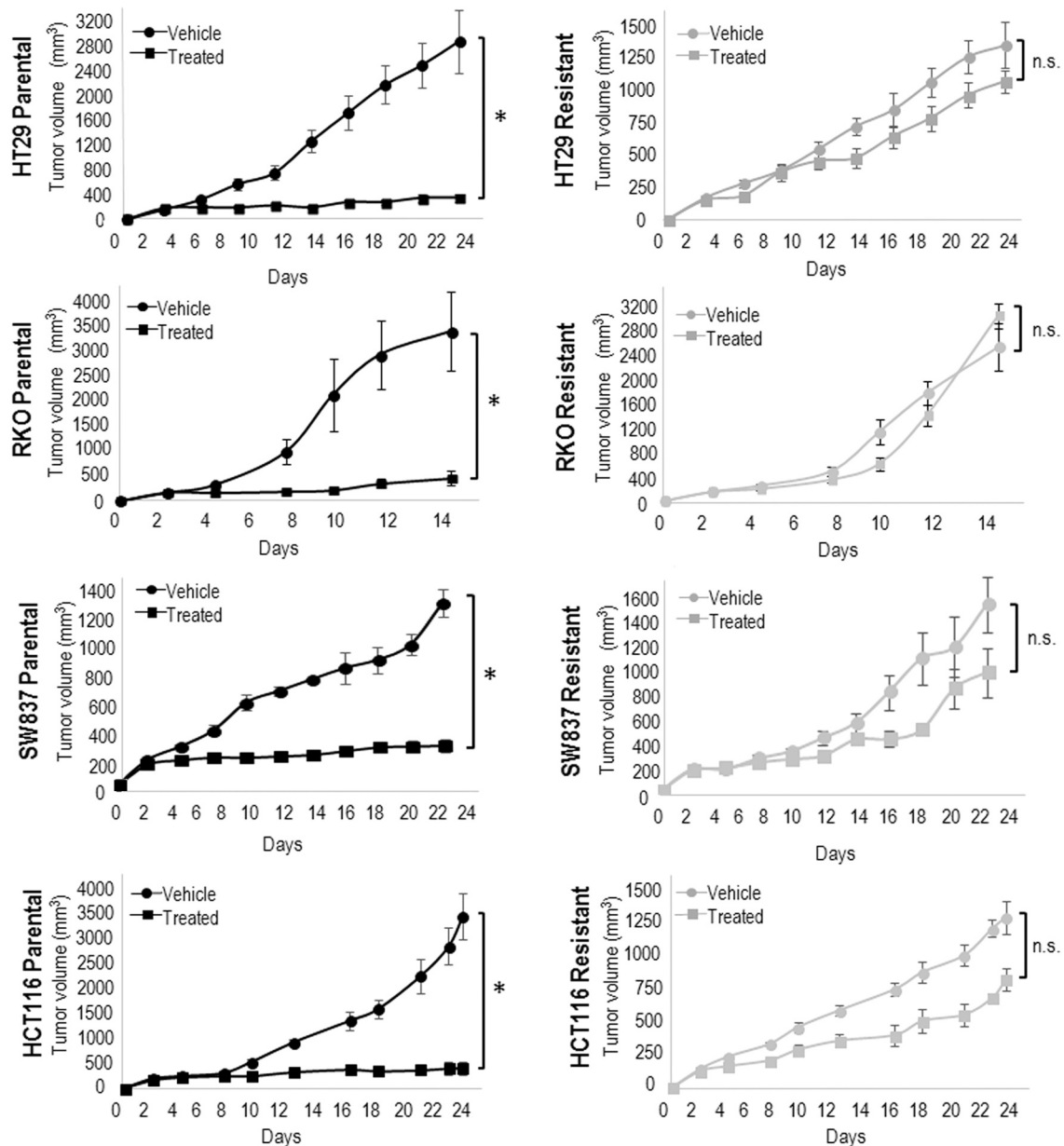
Xenograft model	T/C ratio
HT29	12%
HT29$_R$	80%
RKO	36%
RKO$_R$	119%
SW837	23%
SW837$_R$	64%
HCT116	11%
HCT116$_R$	59%

Fig. 2. *In vivo* validation of BI2536-resistant cell lines. Tumor growth curves of xenograft models developed with parental (HT29 $n = 15$, SW837 $n = 10$, RKO $n = 11$ and HCT116 $n = 10$) (left) and resistant cell lines (HT29$_R$ $n = 14$, SW837$_R$ $n = 10$, RKO$_R$ $n = 12$ and HCT116$_R$ $n = 13$) (right) treated with BI2536 (20 mg/kg) or vehicle. *X* axis represents days from starting treatment and *Y* axis represents tumor volume in mm^3. Each point on line graph represents the mean of tumor volume (mm^3) at a particular day after implantation; bars represent standard deviation (SD). At endpoint, final tumor volumes were compared between treated and non-treated groups. Statistical differences were considered when $p < 0.05$ (*). Table shows T/C ratio values (in percentage) obtained for each model.

IG$_{50}$ were RKO 35 nM and RKO$_R$ 1000 nM; GSK461364 IG$_{50}$ values were RKO 15 nM and RKO$_R$ 150 nM; and GW843682X IG$_{50}$ values were RKO 180 nM and RKO$_R$ 2000 nM, supporting the role of this mutation in the loss of affinity of PLK1 inhibitors to its binding site (Supplementary Figure 2B).
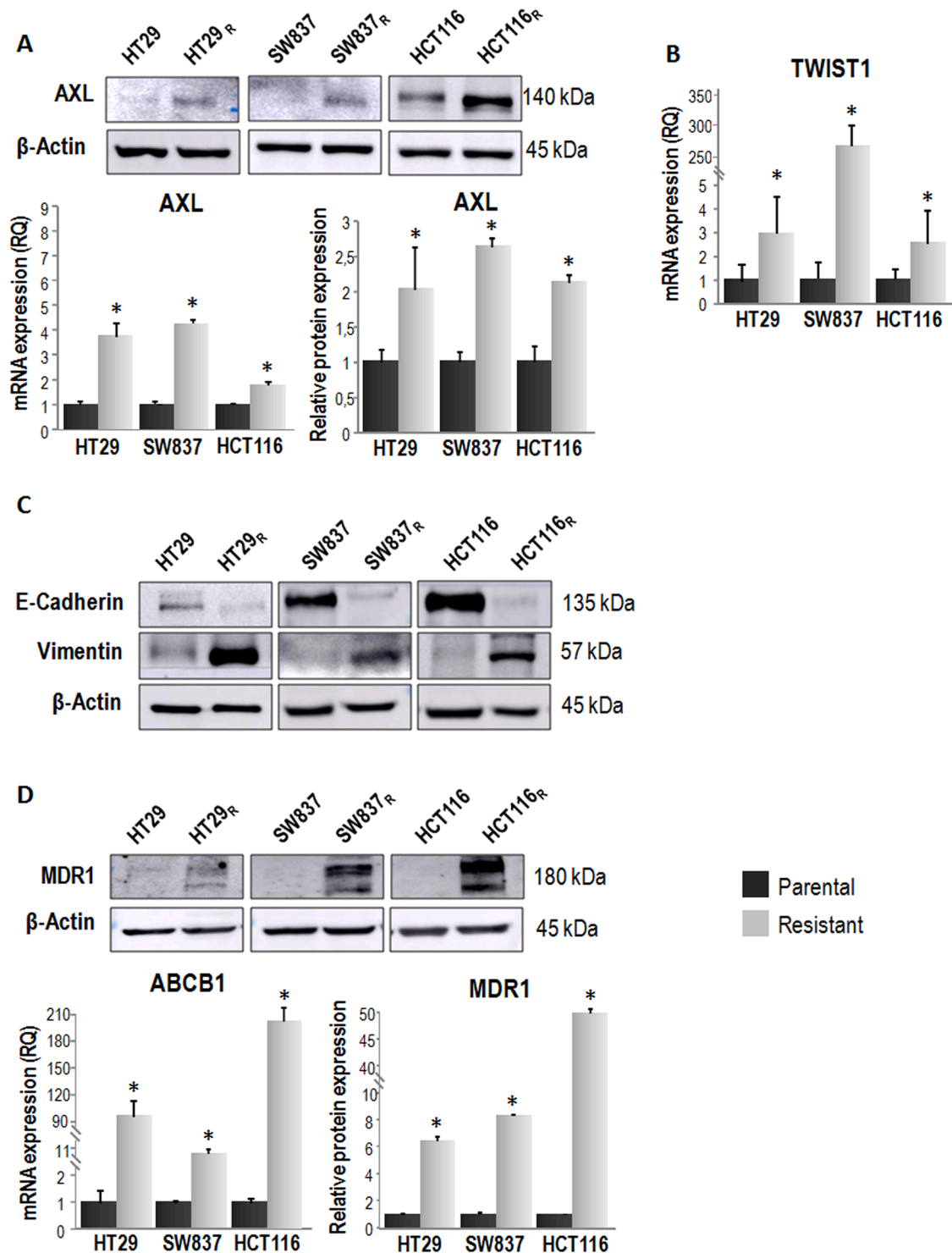
Fig. 3. BI2536-resistant cells activate AXL signaling pathway trough transcription factor TWIST1 overexpression, epithelial-to-mesenchymal transition and MDR1 upregulation. (A) AXL levels of protein and mRNA assessed by western blot and quantitative PCR from parental (black bars) and resistant (grey bars) cell lines. (B) mRNA expression of *TWIST1* by quantitative PCR in resistant (grey bars) lines compared to parental (black bars) lines. (C) Western blots of E-Cadherin and Vimentin in parental (black bars) *versus* resistant (grey bars) cells lines. (D) Western blot and quantitative PCR of MDR1 and *ABCB1*, respectively, in parental (black bars) and resistant (grey bars) cell lines. β-actin is used as a control loading in western blot experiments and *RPLP0* probe was used as housekeeping for qPCR. Data in all graphs are expressed as mean ± SD of 3 independent experiments and represented as relative change with respect to the reference value (parental cells). Statistical differences were considered when p < 0.05 (*).

### 3.3. AXL mediated EMT and MDR1 upregulation via TWIST1 in resistant cells

AXL is a receptor tyrosine kinase largely linked to chemoresistance; many evidences have pointed to AXL as responsible for the development of resistance to anticancer therapies including antimitotic drugs such paclitaxel [25], docetaxel [26], vincristine [27] or even inhibitors related to PLK1 pathway such WEE1 inhibitor, AZD1775 [28]. Its signaling downstream is led by TWIST1, which in turn activates the expression of a gene program potentially responsible of BI2536 resistance through the epithelial-to-mesenchymal transition (EMT) and the transcriptional regulation of *ABCB1* which encodes the multidrug resistance protein MDR1, also known as P-glycoprotein (P-gp).

As part of the characterization of the mechanism involved in the resistance acquisition, AXL, *TWIST1*, E-Cadherin, Vimentin, *ABCB1* and MDR1 expression levels were assessed in BI2536-resistant and parental cell lines without detected mutation (HT29, SW837 and HCT116).

Results showed a significant ($p < 0.05$) upregulation of *AXL* in all resistant cells compared to parental ones; these data also correlated with the protein expression. Thus, PLK1 inhibitor resistance was associated with a significant increase of the AXL receptor (Fig. 3A).

Consequently, we evaluated the expression of *TWIST1*, the transcriptional factor involved in AXL signaling. All resistant cell lines (HT29$_R$, SW837$_R$ and HCT116$_R$) showed significant overexpression of
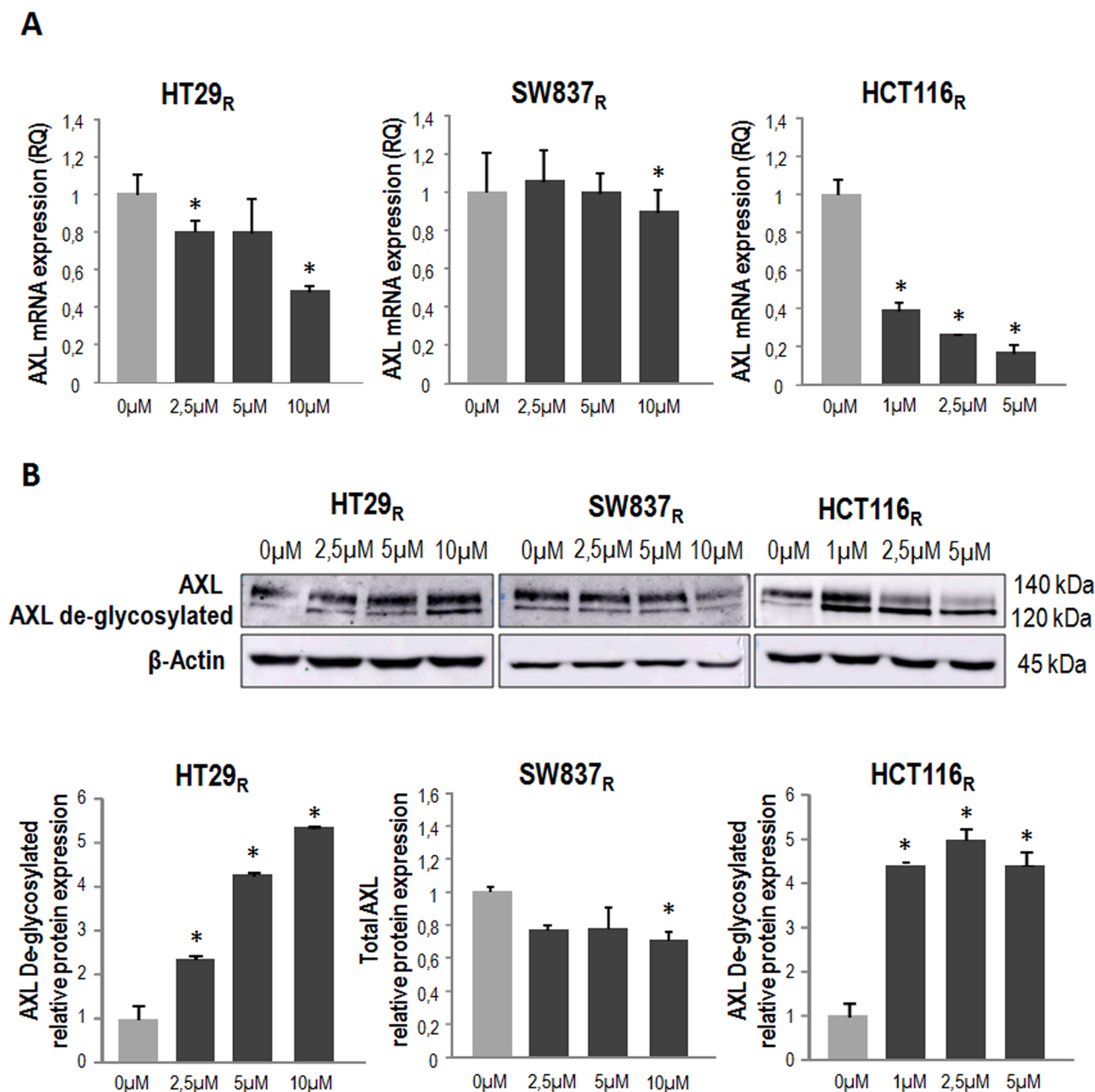
Fig. 4. Simvastatin treatment deregulates AXL in BI2536-resistant cell lines (A) mRNA expression of *AXL* after 48 h of simvastatin treatment in resistant cell lines. Doses used for the experiments were the following: 0 μM (non-treated) (grey bar), 2.5 μM, 5 μM and 10 μM for HT29$_R$ and SW837$_R$ lines, and 1 μM, 2.5 μM and 5 μM for HCT116$_R$ line (black bars). *RPLP0* probe was used as housekeeping for qPCR. (B) AXL protein levels after simvastatin treatment in resistant cell lines. β-actin was used as a control loading. AXL de-glycosylated fraction was quantified in HT29$_R$ and HCT116$_R$ and total protein was quantified in SW837$_R$. Data in all graphs are expressed as mean ± SD of 3 independent experiments and represented as relative change with respect to the reference value (resistant non-treated cells). Statistical differences were considered when $p < 0.05$ (*).

TWIST1 compared to parental cells (Fig. 3B).

TWIST1 is directly related with the epithelial-to-mesenchymal transition, characterized by a loss of epithelial-like proteins (E-Cadherin) towards a gain of mesenchymal markers (Vimentin). Evaluation of these EMT markers by western blot showed that resistant cells had mesenchymal phenotypes compared to their parental partners (Fig. 3C). These results support that the signaling through AXL and TWIST1 drives resistant cells towards a mesenchymal phenotype as part of the acquired resistance mechanism.

AXL has already been related with MDR1 upregulation in resistance cases [29], what explain our evaluation of the multidrug resistance protein 1 (MDR1), which is encoded by *ABCB1*. MDR1 expression was significantly higher in resistant cell lines compared with parental ones both at mRNA and protein level (Fig. 3D). Changes in protein go from 6 to 50-fold in resistant lines, and overexpression observed in mRNA reaches 200-fold compared with parental lines. These results confirm that MDR1 plays a main role in the acquisition of resistance to PLK inhibitors.

To corroborate the key role of AXL axis in resistance mechanism, we interfered AXL signaling treating resistant cells with its inhibitor R428, with doses of 5 μM and 8 μM for HT29$_R$ and HCT116$_R$, and 8 μM and 10 μM for SW837$_R$. Results are shown in Supplementary Figure 3, where we could observe a significative downregulation of *TWIST1*, *Vimentin* and *ABCB1* genes by qPCR and the overexpression of the epithelial marker E-cadherin by western blot in all resistant lines treated with R428, confirming that AXL axis is crucial for resistance mechanism.

3.4. Simvastatin impairs the resistance mechanism induced by BI2536

Statins treatment has already been related with improvement of survival and outcome in patients with resistance to anticancer drugs [30]. Therefore, we investigated the role of statins as potential candidates for targeting BI2536 resistance. The effect of simvastatin on the molecular mechanism induced by acquired-resistance was assessed. We used several doses to test the effect of this inhibitor: 2,5 μM, 5 μM and 10 μM for HT29$_R$ and SW837$_R$ cell lines, and 1 μM, 2,5 μM and 5 μM for HCT116$_R$ cell line. Simvastatin exerted a significant dose-dependent downregulation of *AXL* expression in all resistant cells (Fig. 4A).

Additionally, protein analysis revealed that HT29$_R$ and HCT116$_R$ showed protein de-glycosylation pattern observed by changes in the electrophoretic mobility in a dose-dependent manner after simvastatin treatment (Fig. 4B). SW837$_R$ did not present this pattern, but, in turn, it showed a significant decrease of the total protein when it was treated at 10 μM.

Regarding the signaling downstream AXL, a significant downregulation of *TWIST1* after 48 h of simvastatin treatment was observed in all resistant cells (Fig. 5A). Mesenchymal-to-epithelial transition (MET) was also observed after simvastatin treatment, since all resistant cell lines recovered E-cadherin expression and lost Vimentin (Fig. 5B). In case of MDR1, we evaluated by Multidrug Resistance Activity Assay if simvastatin was able to impair its function, avoiding the drug efflux and contributing to chemosensitization. Cells showed significant increase intracellular amounts of MDR1 substrate Calcein AM in a dose-dependent manner (Fig. 6), suggesting simvastatin was able to inhibit drug-exclusion mediated by MDR1 and therefore producing the accumulation of BI2536 inside cells. All these results point to a simvastatin-mediated impairment of the acquired resistance mechanism.

3.5. Combination of BI2536 and simvastatin re-sensitizes in vitro and in vivo resistant models

To determine whether simvastatin is able to reverse BI2536 resistance, we evaluated the effect of BI2536, simvastatin or the combination of both on the survival of resistant cells. The results showed an additive effect of the combinatorial treatment which significantly decrease the cell viability up to 50% compared with non-treated cells, or with cells treated with the drugs in monotherapy (Fig. 7).

Later, this combinatory therapy was *in vivo* evaluated by developing a xenograft model using HT29$_R$ cell line. When tumors reached 150 mm^3, animals were randomized in four branches (vehicle, BI2536, simvastatin and combination of both) and treated during 21 days. At the end of the experiment, tumor growth and T/C ratios were calculated. Tumors treated with BI2536 or simvastatin as monotherapy showed T/C ratios of 62% and 78%, respectively, confirming their resistant phenotypes. However, T/C ratio of tumors treated with the combinatorial therapy was 37%, confirming the re-sensitizing effect exerted by simvastatin in presence of BI2536 (Fig. 8A).

To explore the molecular resistance mechanism found in resistance and also the ability of simvastatin to reverse that pathway in the xenograft model, tumor samples were processed and analyzed, showing a statistical significant downregulation of *AXL* and its effectors *TWIST1* and *ABCB1* by qPCR in tumors treated with simvastatin and with the combinatorial scheme (Fig. 8B). These data confirmed that simvastatin was able to impair AXL axis also in tumor samples even in monotherapy or in combination with BI2536.

4. Discussion

In spite of CRC diagnosis and survival in early stages have improved, metastatic disease management continues being challenging. New targeted therapies has risen in the last years, launching a new scenario in terms of therapeutical strategies. This is the case of a group of molecules which are able to disturb cell cycle in mitosis by impairing mitotic protein`s action. Among them, PLK1 is a kinase essential for cell cycle and is overexpressed in many tumor entities. Due to its critical role in mitosis there are many research focused on its inhibition and, so far, several inhibitors have been designed and some of them currently undergo clinical trials (BI2536, Volasertib, GSK461364 or GW843682X) but, spite of their high expectations, the observed results are not being as good as expected, due to the activation of alternative mechanisms to bypass PLK1 inhibition. The discovery and management of the resistance mechanisms observed in trials could result in the re-positioning of PLK1 inhibitors leading to improved outcomes.

With this objective in mind, we investigated the resistance mechanisms associated to the continuous exposure to PLK1 inhibitor BI2536 in CRC cell lines. It is well known that mutation acquisition is one of the most effective mechanisms to overcome the inhibition exerted by many types of molecules. Several PLK1 mutations have been already described in resistant cells to PLK1 inhibitors. These data supported our research in this regard, and evidenced the presence of R136G mutation in RKO resistant which blocks the inhibitor union to the ATP-binding pocket [31,32] and explaining the resistant mechanism for this cell line. Additionally, we reported this variant also conferred resistance to other ATP-competitive PLK1 inhibitors.

The R136G mutation only explained the PLK1 inhibitors resistance mechanism in one of the four resistant cell lines, directing our research to the identification of alternative mechanisms involved in the resistance acquisition in the rest of the cell lines. In this regard, we guided our efforts in elucidating these resistance mediators by the assessment of pathways already associated to drug resistance. That is the case of AXL, a tyrosine kinase receptor involved in cellular processes such as proliferation, invasion, migration and survival, whose upregulation has been associated with tumor resistance to anticancer therapies including antimitotic drugs such paclitaxel [25], docetaxel [26], vincristine [27] or even inhibitors related to PLK1 pathway such WEE1 inhibitor, AZD1775 [28,33]. This receptor activates in turn a downstream pathway mediated by TWIST1, a transcriptional factor which has been addressed as the main regulator of several molecular processes which favor the resistance acquisition: epithelial-to-mesenchymal transition (EMT) and the upregulation of the Multidrug Resistance protein MDR1, already described in previous reports to be involved in other drug resistance [26,34–36]. Additionally and supporting this hypothesis,
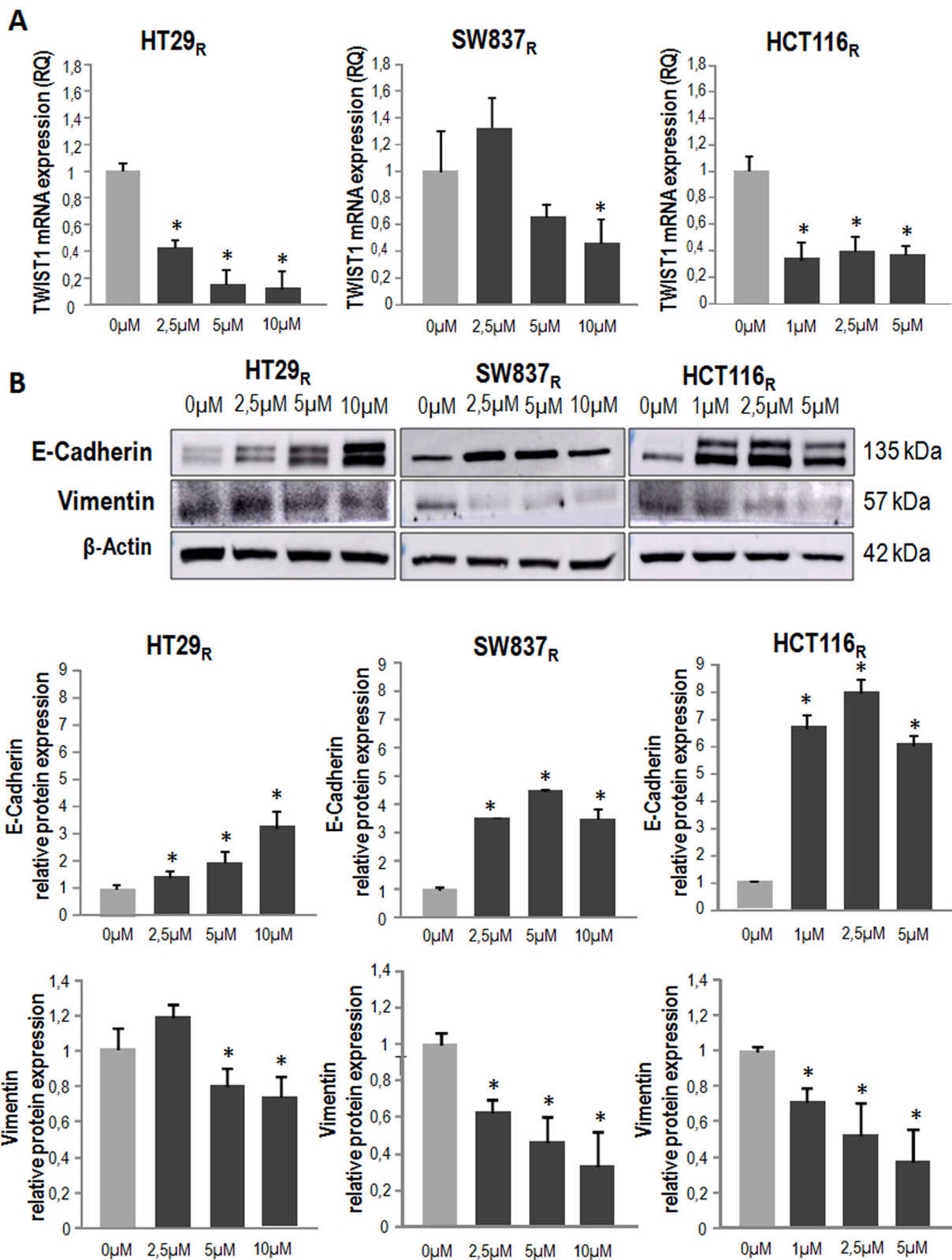
Fig. 5. Simvastatin induces TWIST1 downregulation and reversion of epithelial-to-mesenchymal transition in BI2536-resistant cells. (A) *TWIST1* mRNA expression was evaluated after 48 h of simvastatin treatment. Doses used for the experiments were the following: 0 μM (non-treated) (grey bar), 2.5 μM, 5 μM and 10 μM for HT29$_R$ and SW837$_R$ lines, and 1 μM, 2.5 μM and 5 μM for HCT116$_R$ line (black bars). *RPLP0* probe was used as housekeeping for qPCR. (B) Epithelial-to-mesenchymal transition markers expression, E-Cadherin and Vimentin, was evaluated in resistant cells after simvastatin treatment. β-actin was used as a control loading. Data in all graphs are expressed as mean ± SD of 3 independent experiments and represented as relative change with respect to the reference value (resistant non-treated cells). Statistical differences were considered when $p < 0.05$ (*).
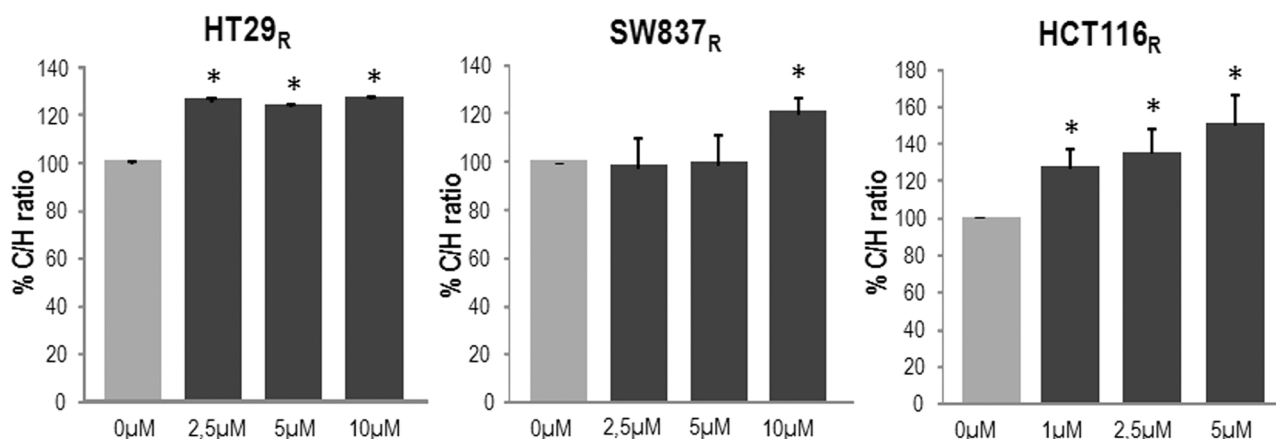
Fig. 6. Simvastatin induces loss of activity of MDR1 in BI2536-resistant cells. MDR1 activity assay was measured by the intracellular fluorescent signal of calcein AM in BI2536-resistant cells treated with increased doses of simvastatin. Doses used for the experiments were the following: 0 μM (non-treated) (grey bar), 2.5 μM, 5 μM and 10 μM for HT29$_R$ and SW837$_R$ lines, and 1 μM, 2.5 μM and 5 μM for HCT116$_R$ line (black bars) Data in all graphs are expressed as mean ± SD of Calcein AM/ Hoechst ratio of 3 independent experiments expressed as percentage with respect to the reference value (resistant non-treated cells). Statistical differences were considered when p < 0.05 (*).
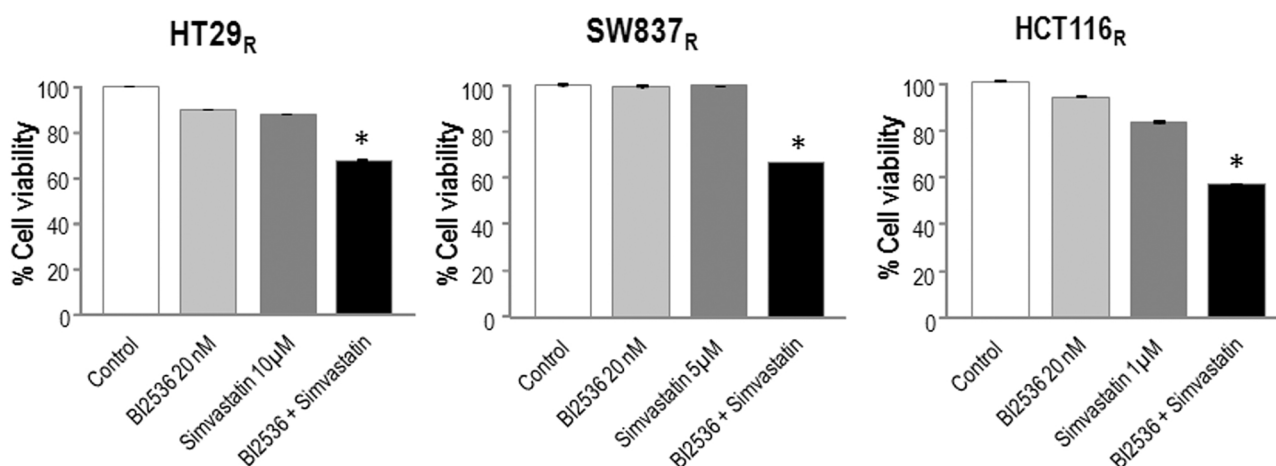
Fig. 7. BI2536 and simvastatin combined decrease resistant cell viability *in vitro*. Cell viability assessment of resistant cells treated for 48 h with RPMI, BI2536 20 nM and simvastatin (HT29$_R$ 10 μM, SW837$_R$ 5 μM and HCT116$_R$ 1 μM) as monotherapy or in combination. Data in all graphs are expressed as mean ± SD of 3 independent experiments and show the percentage of cell viability for each treatment condition (BI2536 and simvastatin in monotherapy (grey bars) and combinatory (black bars)) with respect to the reference value (resistant non-treated cells, white bar). Statistical differences were considered when p < 0.05 (*).

Haupenthal J et al. [37] observed low intratumoral levels of BI2536 in a resistant preclinical model, confirming that the increased drug efflux could be a common resistance mechanism also in the PLK1 inhibitor resistance context.

This study showed that our resistance models shared these mechanisms: increased AXL signaling led the acquisition of BI2536 resistant behavior in HT29$_R$, SW837$_R$ and HCT116$_R$ by means of an overexpression of TWIST1, which contributed, on one hand, to the switched-on of the gene program responsible for the significant decrease of adhesion epithelial proteins (E-cadherin) in parallel to the increase of mesenchymal markers (Vimentin), and on the other hand to the overexpression of *ABCB1* gene which correlated with high levels of MDR1 observed in resistant cells.

Acquired resistance is a common mechanism of tumors to bypass drug-induced blockage and developing combined therapies is essential to re-sensitize tumors and get a better antitumoral response. There are molecules capable to re-sensitize tumors through inhibition of several essential pathways; this is the case of statins which are inhibitors of HMG-CoA reductase (HMGCR), an essential enzyme of mevalonate pathway (MVP). Due to the amount of oncogenic pathways that depend on MVP to carry out its action, statins have already been considered as antitumoral agents because of its function on the inhibition of migration and invasion, proliferation, survival and stemness in cancer cells [38]. With that assumption, the effect of simvastatin on non- mutated BI2536 resistant cells was evaluated. We demonstrated that simvastatin was able to reverse the resistant phenotype by inducing deglycosylation and downregulation of AXL. As a consequence, a disruption of AXL signaling was observed through the negative regulation of TWIST1 that ultimately led to a reversion of the EMT process and an increase in intracellular levels of the drug due to decrease of MDR1 as part of the re-sensitization of BI2536-resistant cells.

It is well known that statins inhibit the HMGCR activity at early stages of mevalonate pathway and indirectly affect a number of intermediate products, including non-sterol isoprenoids. That is the case of dolichol, a molecule responsible for transporting N-glycosylated oligosaccharides residues to a target protein [39]. As it has been already published, AXL needs to be glycosylated to carry out its action [40], having a different molecular weight between 120 and 140 kDa depending on the presence of glycosylated residues. In our experiments, we evidenced a defect in AXL glycosylation in HT29$_R$ and HCT116$_R$, observed as a change in the electrophoretic mobility pattern in a dose-dependent manner. However, SW837$_R$ cell line showed a
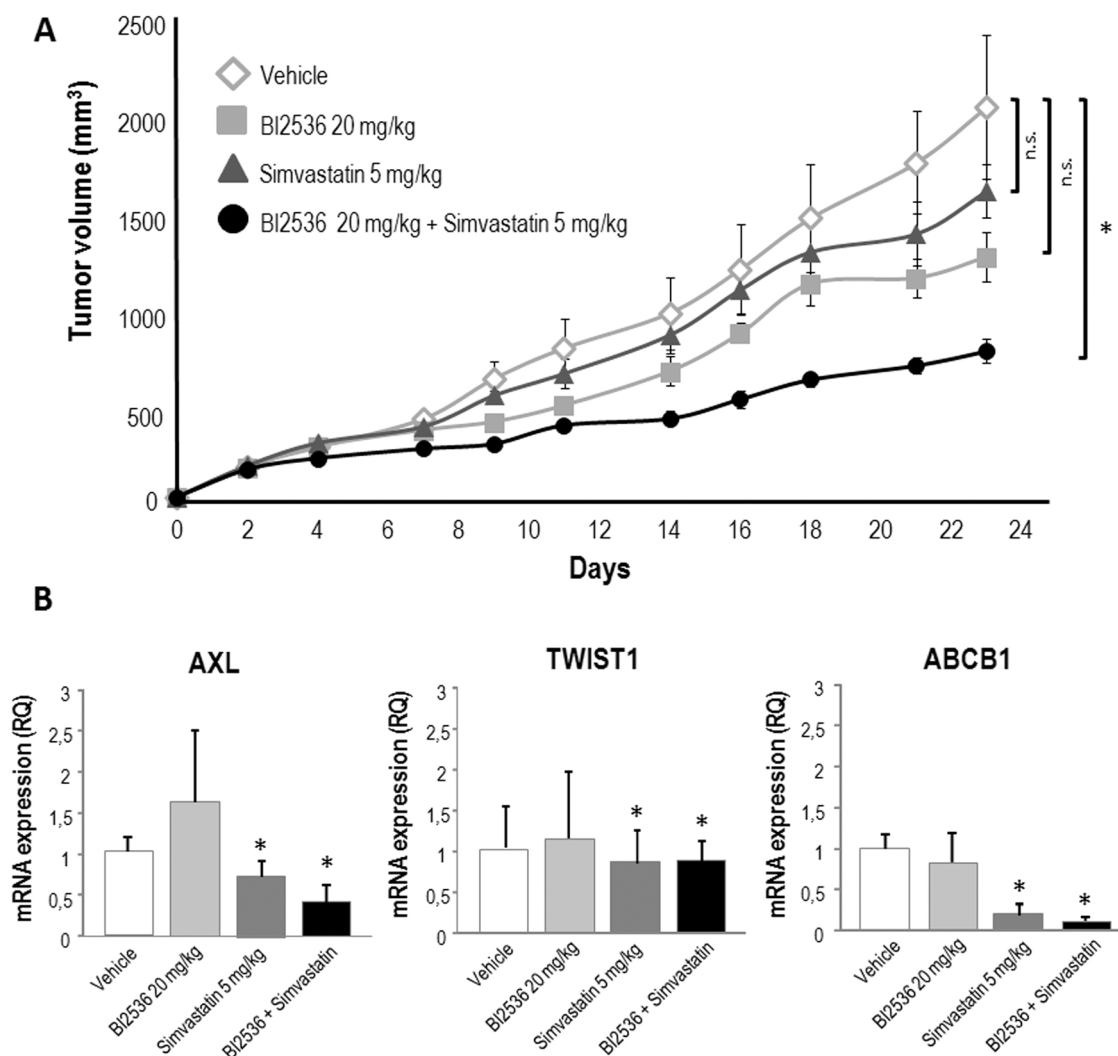
Fig. 8. Simvastatin re-sensitizes resistant cells to BI2536 *in vivo*. (A) Tumor Growth curves of xenografts developed with resistant cell lines treated with vehicle (white line, $n = 5$), BI2536 20 mg/kg ($n = 5$), simvastatin 5 mg/kg ($n = 5$) (grey lines) or BI2536 20 mg/kg + simvastatin 5 mg/kg ($n = 5$) (black lines). *X* axis represents days from starting treatment and *Y* axis represents tumor volume in mm^3. Each point on line graph represents the mean of tumor volume (mm^3) at a particular day after implantation; bars represent standard deviation (SD). At endpoint, final tumor volumes were compared between each treatment and control group. (B) mRNA expression of *AXL*, *TWIST1* and *ABCB1* genes in treated groups compared to control group in tumor samples (BI2536 and simvastatin in monotherapy (grey bars) and combinatory (black bars). Data in all graphs are expressed as mean ± SD of 3 independent experiments. *RPLP0* probe was used as housekeeping for qPCR. Data in bar graph are expressed as mean ± SD of 3 independent experiments. Statistical differences were considered when p < 0.05 (*).

downregulation of total protein level, presumably because of modulations of AXL upstream pathways, caused by isoprenilation defects in proteins as RAS or Rho, as was described by Wang T. et al. [41].

As a consequence of AXL signaling disruption either by defect on its glycosylation or its downregulation, downstream effectors were also altered. This was the case of the transcriptional factor TWIST1, whose levels were reduced to similar levels to the parental cell lines, which involved a restoration of the epithelial phenotype in a similar way to that described in other resistance models [36,42]. The treatment with simvastatin also exerted influence on the functionality of MDR1. We observed by Multidrug Resistance Activity Assay that drug efflux was lower in the treated-resistant cell lines in comparison to non-treated ones. There are several evidences addressing the effect of statins against this pump such as defects in glycosyilation, necessary for its correct function [43], downregulation of *ABCB1* gene [44], or even a direct inhibition of MDR1 by competitive binding of simvastatin to the pump [45]. All these properties make simvastatin a potential re-sensitizer as it has been already described in other contexts such as sorafenib-resistant hepatocellular carcinoma [46], cetuximab-resistant

colorectal cancer [43] and doxorubicin-resistant prostate cancer [44]. This made us wonder if the combination of simvastatin and BI2536 in resistant cells could make them sensitive again. The *in vitro* combination of both drugs produced a decrease in cell viability of up to 50% compared to monotherapy treatments, and the *in vivo* combinatorial therapy caused a relevant inhibition of tumor growth, getting a T/C ratio of 37%. These results confirm that simvastatin acts as a re-sensitizer of BI2536-resistant tumors.

In conclusion, resistance to antitumor agents continues being a critical issue in CRC patient's treatment, pointing to the importance of establishing new strategies to reverse the activated mechanisms or even to prevent their activation. Such is the case of PLK1 inhibitors, promising drugs with a current limited clinical use due to resistance mechanisms; in this scenario, we demonstrated that AXL pathway through increasing TWIST1 transcription factor causes the activation of the EMT process and the MDR1 upregulation as part of the resistance mechanism generated in our cell lines, being simvastatin able to reverse this phenotype, as it has been summarized in Fig. 9. Simvastatin is currently used for lipid malignances as a lipid-lowering agent, interfering in
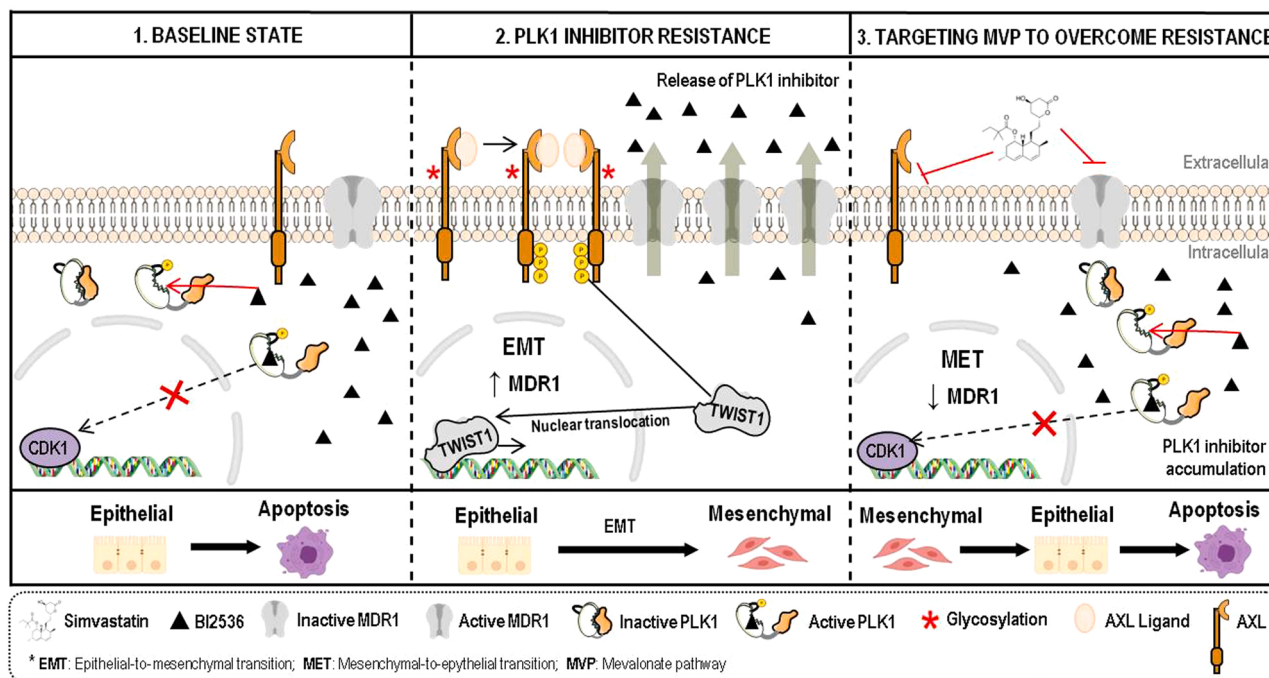
Fig. 9. Schematic resistance mechanism overview. (1) In baseline state CRC cells are sensitive to BI2536 showing an epithelial phenotype due to AXL and MDR1 normal levels, accumulation of the drug inside cells and mitosis impair triggering apoptosis through PLK1 inhibition. (2) When BI2536-resistance is established, increased AXL levels produces an upregulation of *TWIST1*, one of the responsible for the transition from epithelial to mesenchymal phenotype and the increase of MDR1 pump releasing drug out of the cell. (3) The re-sensitization to BI2536 through combination with simvastatin treatment provokes the inactivation of AXL and its downstream pathway, with a loss of TWIST1 and the reversion from mesenchymal to epithelial phenotype as well as inactivation of MDR1 and therefore BI2536 intracellular accumulation, triggering apoptosis again by inhibiting PLK1 when combinatorial treatment is applied.

several metabolic pathways, making defects in cell metabolism, among other effects, which impairs post-transcriptional changes of a high range of proteins necessary for tumor survival and development.

These findings open doors to the use of statins as drugs for overcoming resistance in this context and also in others, being a new tool to be deeply explored in the resistance management due to their relevance in colorectal cancer outcome and treatment.

5. Conclusions

Adaptive resistance mechanisms hamper the efficacy of novel molecules with high therapeutic potential as PLK1 inhibitors. Addressing the resistance mechanisms is crucial to understand the molecular basis of this phenomenon and establishing new therapeutic schemes to overcome it could result in enhanced drug responses. Our findings revealed the mechanisms activated in colorectal cancer cells resistant to PLK1 inhibition and support the use of simvastatin, an inhibitor of mevalonate pathway, as a tool for overcoming the resistance induced by PLK1 inhibitors. This study opens a door for the re-positioning of these inhibitors in the management of metastatic colorectal cancer by its combinatorial use with simvastatin; however, further studies are needed to confirm and extend these promising results.

Author contributions

SSC, LDP and AC wrote the manusctipt. LDP, AC and JGF conceived and designed the experiments. SSC, IM, LGG, ARV, GDC and AMV researched data. MRR, NB, VC, MJFA and JGF contributed to discussion and reviewed/edited the manuscript. All authors approved the final version of the manuscript.

CRediT authorship contribution statement

SSC, LDP and AC wrote the manuscript. LDP, AC and JGF conceived and designed the experiments. SSC, IM, LGG, ARV, GDC and AMV researched data. MRR, NB, VC, MJFA and JGF contributed to discussion and reviewed/edited the manuscript. All authors approved the final version of the manuscript.

Conflict of interest statement

The authors have reported that they have no conflicts of interest, relevant to the contents of this paper, to disclose.

Appendix A. Supporting information

Supplementary data associated with this article can be found in the online version at doi:10.1016/j.biopha.2021.112347.

References

[1] H. Sung, J. Ferlay, R.L. Siegel, M. Laversanne, I. Soerjomataram, A. Jemal, F. Bray, Global cancer statistics 2020: GLOBOCAN estimates of incidence and mortality worldwide for 36 cancers in 185 countries, CA Cancer J. Clin. 71 (2021) 209–249.
[2] O.K. Glebov, L.M. Rodriguez, K. Nakahara, J. Jenkins, J. Cliatt, C.-J. Humbyrd, J. DeNobile, P. Soballe, R. Simon, G. Wright, P. Lynch, S. Patterson, H. Lynch, S. Gallinger, A. Buchbinder, G. Gordon, E. Hawk, I.R. Kirsch, Distinguishing right from left colon by the pattern of gene expression, Cancer Epidemiol. Biomark. Prev. 12 (8) (2003) 755–762.

[3] A. Rowan, S. Halford, M. Gaasenbeek, Z. Kemp, O. Sieber, E. Volikos, E. Douglas, H. Fiegler, N. Carter, I. Talbot, A. Silver, I. Tomlinson, Refining molecular analysis in the pathways of colorectal carcinogenesis, Clin. Gastroenterol. Hepatol. 3 (11) (2005) 1115–1123.

[4] G. Lech, R. Słotwiński, M. Słodkowski, I.W. Krasnodębski, Colorectal cancer tumour markers and biomarkers: recent therapeutic advances, World J. Gastroenterol. 22 (5) (2016) 1745–1755.

[5] J.M. Loree, A.A.L. Pereira, M. Lam, A.N. Willauer, K. Raghav, A. Dasari, V. K. Morris, D.G. Menter, C. Eng, K. Shaw, R. Broaddus, M.J. Routbort, Y. Liu, J.S. Morris, R. Luthra, F. Meric-Bernstam, M.J. Overman, D. Maru, S. Kopetz, Classifying colorectal cancer by tumor location rather than sidedness highlights a continuum in mutation profiles and consensus molecular subtypes, Clin. Cancer Res. 24 (5) (2018) 1062–1072.

[6] R. Labianca, B. Nordlinger, G.D. Beretta, S. Mosconi, M. Mandalà, A. Cervantes, D. Arnold, G. ESMO Guidelines Working, Early colon cancer: ESMO Clinical Practice Guidelines for diagnosis, treatment and follow-up, Ann. Oncol. 24 (Suppl 6) (2013) 64–72, vi64-72.

[7] E. Van Cutsem, A. Cervantes, B. Nordlinger, D. Arnold, ESMO Guidelines Working Group. Metastatic colorectal cancer: ESMO Clinical Practice Guidelines for diagnosis, treatment and follow-up, Ann. Oncol. 25 (Suppl 3) (2014) 1–9, iii1-9.

[8] R.M. McQuade, V. Stojanovska, J.C. Bornstein, K. Nurgali, Colorectal cancer chemotherapy: the evolution of treatment and new approaches, Curr. Med Chem. 24 (15) (2017) 1537–1557.

[9] D.P. Modest, S. Pant, A. Sartore-Bianchi, Treatment sequencing in metastatic colorectal cancer, Eur. J. Cancer 109 (2019) 70–83.

[10] T. Otto, P. Sicinski, Cell cycle proteins as promising targets in cancer therapy, Nat. Rev. Cancer 17 (2) (2017) 93–115.

[11] R. Pellegrino, D.F. Calvisi, S. Ladu, V. Ehemann, T. Staniscia, M. Evert, F. Dombrowski, P. Schirmacher, T. Longerich, Oncogenic and tumor suppressive roles of polo-like kinases in human hepatocellular carcinoma, Hepatology 51 (3) (2010) 857–868.

[12] Z. Liu, Q. Sun, X. Wang, PLK1, a potential target for cancer therapy, Transl. Oncol. 10 (1) (2017) 22–32.

[13] K. Strebhardt, Multifaceted polo-like kinases: drug targets and antitargets for cancer therapy, Nat. Rev. Drug Discov. 9 (8) (2010) 643–660.

[14] I.A. Asteriti, F. De Mattia, G. Guarguaglini, Cross-talk between AURKA and Plk1 in mitotic entry and spindle assembly, Front Oncol. 5 (2015) 283.

[15] S. Schmucker, I. Sumara, Molecular dynamics of PLK1 during mitosis, Mol. Cell Oncol. 1 (2) (2014), e954507.

[16] I. Elsayed, X. Wang, PLK1 inhibition in cancer therapy: potentials and challenges, Future Med. Chem. 11 (12) (2019) 1383–1386.

[17] S.-B. Shin, S.-U. Woo, H. Yim, Differential cellular effects of Plk1 inhibitors targeting the ATP-binding domain or polo-box domain, J. Cell Physiol. 230 (12) (2015) 3057–3067.

[18] M. Dufies, D. Ambrosetti, S. Boulakirba, A. Calleja, C. Savy, N. Furstoss, M. Zerhouni, J. Parola, L. Aira-Diaz, S. Marchetti, F. Orange, S. Lacas-Gervais, F. Luciano, A. Jacquel, G. Robert, G. Pagès, P. Auberger, ATP-competitive Plk1 inhibitors induce caspase 3-mediated Plk1 cleavage and activation in hematopoietic cell lines, Oncotarget 9 (13) (2018) 10920–10933.

[19] Clinical Trials [Internet] https://clinicaltrials.gov.

[20] M.E. Burkard, A. Santamaria, P.V. Jallepalli, Enabling and disabling polo-like kinase 1 inhibition through chemical genetics, ACS Chem. Biol. 7 (6) (2012) 978–981.

[21] D. Sinha, P.H.G. Duijf, K.K. Khanna, Mitotic slippage: an old tale with a new twist, Cell Cycle 18 (1) (2019) 7–15.

[22] E. Komlodi-Pasztor, D.L. Sackett, A.T. Fojo, Inhibitors targeting mitosis: tales of how great drugs against a promising target were brought down by a flawed rationale, Clin. Cancer Res 18 (1) (2012) 51–63.

[23] T.H. Corbett, K. White, L. Polin, J. Kushner, J. Paluch, C. Shih, C.S. Grossman, Discovery and preclinical antitumor efficacy evaluations of LY32262 and LY33169, Invest N. Drugs 21 (1) (2003) 33–45.

[24] C.P. Giacomini, S.Y. Leung, X. Chen, S.T. Yuen, Y.H. Kim, E. Bair, J.R. Pollack, A gene expression signature of genetic instability in colon cancer, Cancer Res 65 (20) (2005) 9200–9205.

[25] M.L. Palisoul, J.M. Quinn, E. Schepers, I.S. Hagemann, L. Guo, K. Reger, A. R. Hagemann, C.K. McCourt, P.H. Thaker, M.A. Powell, D.G. Mutch, K.C. Fuh, Inhibition of the receptor tyrosine kinase AXL restores paclitaxel chemosensitivity in uterine serous cancer, Mol. Cancer Ther. 16 (12) (2017) 2881–2891.

[26] J.-Z. Lin, Z.-J. Wang, W. De, M. Zheng, W.-Z. Xu, H.-F. Wu, A. Armstrong, J.G. Zhu, Targeting AXL overcomes resistance to docetaxel therapy in advanced prostate cancer, Oncotarget 8 (25) (2017) 41064–41077.

[27] A.K. Keating, G.K. Kim, A.E. Jones, A.M. Donson, K. Ware, J.M. Mulcahy, D. B. Salzberg, N.K. Foreman, X. Liang, A. Thorburn, D.K. Graham, Inhibition of Mer and Axl receptor tyrosine kinases in astrocytoma cells leads to increased apoptosis and improved chemosensitivity, Mol. Cancer Ther. 9 (5) (2010) 1298–1307.

[28] T. Sen, P. Tong, L. Diao, L. Li, Y. Fan, J. Hoff, J.V. Heymach, J. Wang, L.A. Byers, Targeting AXL and mTOR pathway overcomes primary and acquired resistance to WEE1 inhibition in small-cell lung cancer, Clin. Cancer Res. 23 (20) (2017) 6239–6253.

[29] P.-A. Nguyen, C.-C. Chang, C.J. Galvin, Y.-C. Wang, S.Y. An, C.-W. Huang, Y. H. Wang, M.H. Hsu, Y.C. Li, H.C. Yang, Statins use and its impact in EGFR-TKIs resistance to prolong the survival of lung cancer patients: a cancer registry cohort study in Taiwan, Cancer Sci. 111 (8) (2020) 2965–2973.

[30] Y. Adachi, Y. Ishikawa, H. Kiyoi, Identification of volasertib-resistant mechanism and evaluation of combination effects with volasertib and other agents on acute myeloid leukemia, Oncotarget 8 (45) (2017) 78452–78465.

[31] P.J. Scutt, M.L.H. Chu, D.A. Sloane, M. Cherry, C.R. Bignell, D.H. Williams, P. A. Eyers, Discovery and exploitation of inhibitor-resistant aurora and polo kinase mutants for the analysis of mitotic networks, J. Biol. Chem. 284 (23) (2009) 15880–15893.

[32] M.L. Palisoul, J.M. Quinn, E. Schepers, I.S. Hagemann, L. Guo, K. Reger, A. R. Hagemann, C.K. McCourt, P.H. Thaker, M.A. Powell, D.G. Mutch, K.C. Fuh, Inhibition of the receptor tyrosine kinase AXL restores paclitaxel chemosensitivity in uterine serous cancer, Mol. Cancer Ther. 16 (12) (2017) 2881–2891.

[33] R. Li, C. Wu, H. Liang, Y. Zhao, C. Lin, X. Zhang, C. Ye, Knockdown of TWIST enhances the cytotoxicity of chemotherapeutic drugs in doxorubicin-resistant HepG2 cells by suppressing MDR1 and EMT, Int. J. Oncol. 53 (4) (2018) 1763–1773.

[34] H.S. Choi, Y.-K. Kim, P.-Y. Yun, Upregulation of MDR- and EMT-related molecules in cisplatin-resistant human oral squamous cell carcinoma cell lines, Int. J. Mol. Sci. 20 (2019) 12.

[35] J. De Las Rivas, A. Brozovic, S. Izraely, A. Casas-Pais, I.P. Witz, A. Figueroa, Cancer drug resistance induced by EMT: novel therapeutic strategies, Arch. Toxicol. 95 (2021) 2279–2297.

[36] J. Haupenthal, V. Bihrer, H. Korkusuz, O. Kollmar, C. Schmithals, S. Kriener, K. Engels, T. Pleli, A. Benz, M. Canamero, T. Longerich, B. Kronenberger, S. Richter, O. Waidmann, T.J. Vogl, S. Zeuzem, A. Piiper, Reduced efficacy of the Plk1 inhibitor BI 2536 on the progression of hepatocellular carcinoma due to low intratumoral drug levels, Neoplasia 14 (5) (2012) 410–419.

[37] F. Iannelli, R. Lombardi, M.R. Milone, B. Pucci, S. De Rienzo, A. Budillon, F. Bruzzese, Targeting mevalonate pathway in cancer treatment: repurposing of statins, Recent Pat. Anticancer Drug Discov. 13 (2) (2018) 184–200.

[38] M. Welti, Regulation of dolichol-linked glycosylation, Glycoconj. J. 30 (1) (2013) 51–56.

[39] N. Lee, W.-J. Jang, J.H. Seo, S. Lee, C.-H. Jeong, 2-deoxy-d-glucose-induced metabolic alteration in human oral squamous SCC15 cells: involvement of N-glycosylation of Axl and met, Metabolites 9 (2019) 9.

[40] T. Wang, S. Seah, X. Loh, C.-W. Chan, M. Hartman, B.-C. Goh, S.C. Lee, Simvastatin-induced breast cancer cell death and deactivation of PI3K/Akt and MAPK/ERK signalling are reversed by metabolic products of the mevalonate pathway, Oncotarget 7 (3) (2016) 2532–2544.

[41] E. Kaşıkcı, E. Aydemir, Ö.F. Bayrak, F. Şahin, Inhibition of migration, invasion and drug resistance of pancreatic adenocarcinoma cells - role of snail, slug and twist and small molecule inhibitors, Onco Targets Ther. 13 (2020) 5763–5777.

[42] P. Jiang, R. Mukthavavam, Y. Chao, I.S. Bharati, V. Fogal, S. Pastorino, X. Cong, N. Nomura, M. Gallagher, T. Abbasi, S. Vali, S.C. Pingle, M. Makale, S. Kesari, Novel anti-glioblastoma agents and therapeutic combinations identified from a collection of FDA approved drugs, J. Transl. Med. 12 (2014) 13.

[43] S. Mallappa, P.K. Neeli, S. Karnewar, S. Kotamraju, Doxorubicin induces prostate cancer drug resistance by upregulation of ABCG4 through GSH depletion and CREB activation: relevance of statins in chemosensitization, Mol. Carcinog. 58 (7) (2019) 1118–1133.

[44] E. Wang, C.N. Casciano, R.P. Clement, W.W. Johnson, HMG-CoA reductase inhibitors (statins) characterized as direct inhibitors of P-glycoprotein, Pharm. Res. 18 (6) (2001) 800–806.

[45] J. Feng, W. Dai, Y. Mao, L. Wu, J. Li, K. Chen, Q. Yu, R. Kong, S. Li, J. Zhang, J. Ji, J. Wu, W. Mo, X. Xu, C. Guo, Simvastatin re-sensitizes hepatocellular carcinoma cells to sorafenib by inhibiting HIF-1α/PPAR-γ/PKM2-mediated glycolysis, J. Exp. Clin. Cancer Res. 39 (1) (2020) 24.

[46] J. Lee, I. Lee, B. Han, J.O. Park, J. Jang, C. Park, W.K. Kang, Effect of simvastatin on cetuximab resistance in human colorectal cancer with KRAS mutations, J. Natl. Cancer Inst. 103 (8) (2011) 674–688.